Journal of Biomedical Optics 6(1), 14–22 (January 2001)

Automated single-cell sorting system based on optical trapping

S. C. Grover
University of Toronto
Faculty of Medicine
1 King's College Circle
Toronto, Ontario, Canada M5S 1A8

A. G. Skirtach
National Research Council
Institute for National Measurement Standards
1500 Montreal Road
Ottawa, Ontario, Canada K1A 0R6

R. C. Gauthier
Laurentian University
Department of Physics and Astronomy
Ramsay Lake Road
Sudbury, Ontario, Canada P3E 2C6

C. P. Grover
National Research Council
Institute for National Measurements Standards
1500 Montreal Road
Ottawa, Ontario, Canada K1A 0R6

Abstract. We provide a basis for automated single-cell sorting based on optical trapping and manipulation using human peripheral blood as a model system. A counterpropagating dual-beam optical-trapping configuration is shown theoretically and experimentally to be preferred due to a greater ability to manipulate cells in three dimensions. Theoretical analysis performed by simulating the propagation of rays through the region containing an erythrocyte (red blood cell) divided into numerous elements confirms experimental results showing that a trapped erythrocyte orients with its longest axis in the direction of propagation of the beam. The single-cell sorting system includes an image-processing system using thresholding, background subtraction, and edge-enhancement algorithms, which allows for the identification of single cells. Erythrocytes have been identified and manipulated into designated volumes using the automated dual-beam trap. Potential applications of automated single-cell sorting, including the incorporation of molecular biology techniques, are discussed.
 [DOI: 10.1117/1.1333676]

Keywords: optical trapping; optical tweezers; single-cell sorting; cell separation; lab-on-a-chip.

Paper JBO 90048 received Sep. 9, 1999; revised manuscript received Oct. 9, 2000; accepted for publication Oct. 25, 2000.

1 Introduction

Optical trapping, first reported by Ashkin in 1970,[1] is a purely optical technique that takes advantage of the radiation pressure exerted by one or more focused laser beams on a microscopic particle. A focused light beam imparts two major categories of forces upon objects in its path. The *scattering force*, which is a consequence of the change in momentum of photons scattered off the surface of the object, acts in the direction of the beam propagation. Two counterpropagating beams can thus act as a stable trap for a particle, provided that the forces acting in the direction of propagation of each beam are equal and are able to overcome forces that tend to drive the particle out of the trapping region. The *gradient force* acts proportional to and in the same direction as the spatial gradient in light intensity caused by focusing the beam, and is derived from fluctuating electric dipoles induced when light passes through a transparent or near-transparent object. Photons with a given momentum are refracted through the dielectric object with a given index of refraction greater than that of the outside medium. The change of momentum in the refracted photon causes an equal and opposite change in the momentum of the object, imparting a force on the object equal to the net rate of change of momentum of all refracted photons. As this gradient force tends to draw objects toward regions of greater light intensity, a particle can be stably trapped in the focus of a single beam of light if this gradient force is sufficient to overcome forces that tend to drive it out of the focus.[2]

The single-beam gradient-force optical trap, termed *optical tweezers*, was first achieved in 1986.[3] Ashkin et al. were the first to conjecture and demonstrate the use of optical tweezers in biological applications, including the manipulation of single cells.[4] Since then, optical tweezers have found a niche in a variety of research applications, including the assessment of the physics of mechanoenzymes,[5,6] micromanipulation for cell fusion and microsurgery,[7,8] single sperm micromanipulation,[9] studies on vesicle motility,[10] and developmental studies on ciliated cells.[11] The technology is also suited for applications in medical diagnostics and therapy, fields in which it has yet to be well exploited.

We provide a basis for an all-optical automated single-cell sorting system based upon single- and dual-beam optical-trap configurations. Single-cell sorting is defined as the compartmentalization of a heterogeneous mixture of particles of types 1 to n into designated volumes V_1 to V_n, and is of unique importance as a tool in research in cell biology, immunology, and genetics,[12] as well as in medical therapeutic strategies, such as cellular therapy.[13] Micromanipulation of single cells is readily attained by optical trapping due to the ease of focusing a laser beam or multiple laser beams onto a spot that is of the same size as a single cell. The algorithmic components of such a microrobotic single-cell sorter are the following: (1) identification of the cell to be sorted, by morphological or other means; (2) trapping of the cell; and (3) manipulation of the cell into a designated volume. Automation of such a system can be attained provided that cell identification and manipulation of the optical system can be performed by computer.[14] Human peripheral blood, composed of three cel-

Address all correspondence to C. P. Grover. Tel: +1-613-993-2098; Fax: +1-613-954-3338; E-mail: chander.grover@nrc.ca

1083-3668/2001/$15.00 © 2001 SPIE

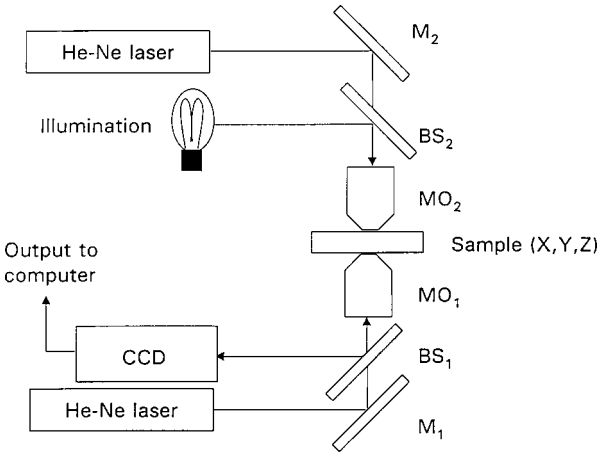

Fig. 1 Optical setup for the dual-beam trap. Two cw He–Ne ($\lambda = 632.8$ nm) laser beams are directed onto the sample from the top and bottom, respectively, with white-light illumination from the top. M, mirror; BS, beamsplitter; MO1, 40× 0.65 NA microscope objective; MO2, 20× 0.45 NA microscope objective; and CCD, color CCD camera. The single-beam trap used is obtained by turning off laser L2 and using a 100×, 1.25 NA microscope objective as MO1.

lular constituents—erythocytes (red blood cells), leukocytes (white blood cells), and platelets—was used as a model system, as cellular identification based upon morphological characteristics is possible. Theoretical analysis of the trapping of erythrocytes, the most common constituent of peripheral blood, was first performed through the use of optical-trapping modeling programs, in order to predict the behavior of erythrocytes in the optical-trapping systems during manipulation. In addition, applications of this technology in medical diagnostics, therapy, and research are discussed.

2 Optical Setup and Sample Preparation

The basic design of the optical-trap systems used is shown in Figure 1. This setup involves the use of two counterpropagating laser beams (He–Ne; $\lambda = 632.8$ nm), which are focused onto the sample, from the top using a 40× 0.45 NA objective (MO1) and from the bottom using a 20× 0.65 NA objective (MO2), respectively. Illumination with white light was achieved through the top microscope objective MO2. This dual-beam optical-trapping system is based on the use of the scattering forces exerted by each of the two counterpropagating beams through low-magnification microscope objectives. It is independent of the spatial gradient in beam intensity; and, as a result, the use of high-magnification, high-numerical-aperture objectives is not required in order to focus the laser beams.

Experiments were also performed using a single-beam trapping configuration, where laser L1 is not used and the lower microscope objective lens MO1 is changed to one of high-magnification and high-numerical aperture (100× 1.25 NA). An Ar-ion laser ($\lambda = 514.5$ nm) was also used as L2 in the single-beam configuration to increase the power density and investigate the effects of local heating in the focus of the microscope objective. Sample holders consisted of two 150-μm-thick glass coverslips separated by a 150-μm-thick Mylar film spacer. Blood samples were obtained from willing human donors and were diluted 1:100 000 in 0.9% saline containing 1 g/L bovine serum albumin (Sigma), to prevent formation of echinocytes and adherence of cells.[15] Styrene divinylbenzene latex microspheres (Dow Chemicals) of diameter 7–14 μm were used in the calibration of the traps.

Sample holders were fitted with motorized X, Y, and Z stages controlled by a computer and an imaging system was incorporated into the laser delivery optics of the traps. Video output was relayed to a computer program fitted with algorithms for the identification and positioning of blood cells, which activated the motorized stages to direct the beams onto the sample. The XY plane was identified as the plane of imaging, and the Z axis was identified as the axis perpendicular to this. The entire trapping system allows for computerized identification and subsequent manipulation of cells for sorting.

3 Theoretical Determination of Erythrocyte Behavior in an Optical-Trapping System

For the purpose of modeling, the shape of the erythrocyte was approximated as a biconcave disk,[16] with a maximum diameter of 7.2 μm, a maximum thickness of 2.1 μm, and a minimum thickness of 0.9 μm,[17,18] and specific gravity of 1.057 g/ml.[19] The forces exerted on each cell can be calculated by summing all the force elements produced by the interaction of photons with the cell surface. Each force element is comprised of scattering (SC) and gradient (GR) components.[20,21] Each reflection or refraction from the cell can be interpreted as scattering from a spherical surface provided that the angle of refraction or reflection is coordinate dependent. Equations for the forces acting on the erythrocyte can then be expressed in a form similar to that for spheres:[20,21]

$$F_{\mathrm{SC}} = \frac{n_M I}{c}\left\{1 + R\cos[2\vartheta(\mathbf{r}_i)] + \left(1 + m\sum_{n=0}^{\infty} T^{2n}\right) T^2 \sum_{n=0}^{\infty} R^n \cos[\alpha(\mathbf{r}_i) + n\beta(\mathbf{r}_i)]\right\}, \tag{1}$$

$$F_{\mathrm{GR}} = \frac{n_M I}{c}\left\{R\sin[2\vartheta(\mathbf{r}_i)] + \left(1 + m\sum_{n=0}^{\infty} T^{2n}\right) T^2 \sum_{n=0}^{\infty} R^n \sin[\alpha(\mathbf{r}_i) + n\beta(\mathbf{r}_i)]\right\}, \tag{2}$$

where n_M is the refractive index of the medium, I is the total intensity, c is velocity of light, θ is the angle of incidence, $\mathbf{r}_i$ is the spatial coordinate (x_i, y_i, z_i), and R and T are reflection and transmission coefficients, respectively. Angles α and β are defined in Figure 2. The term containing the factor m accounts for the possibility of photons reentering the cell due to its biconcave shape. Internal reflections account for approximately 3% of the force induced on a particle and can, in general, be neglected in calculations.[21]

Simulations were performed for the dual-beam trapping configuration with a laser power of 15 mW for the top beam

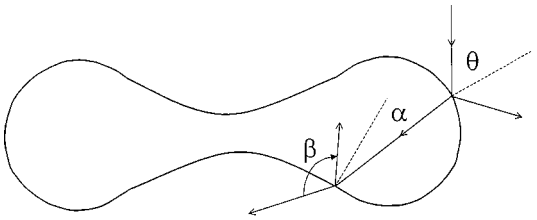

Fig. 2 Schematic of erythrocyte showing angle of incidence (θ) and angles α and β, as defined for modeling studies.

and 30 mW for the bottom beam. The beam diameters were taken to be 5 μm. Numerical calculations were performed by dividing the erythrocyte's surface into 1024 triangular elements and propagating up to 6000 rays through the region containing the cell. The torque about the center of the cell that induces it to rotate and align in the optical trap[22] was calculated by summing over all of the elements, and is shown as a function of the angle of orientation of the cell in Figure 3. Unstable equilibrium orientations for the erythrocyte are found to be at 90° and 270°, and stable equilibrium orientations are at 0°, 180°, and 360°. Subjected to the total radiation force, an erythrocyte is centered in the beam. This can be clearly seen in Figure 4, which shows the results of theoretical modeling (top row) of an erythrocyte orientation in a dual-beam optical-trapping system by propagation of rays through the region containing the cell. An erythrocyte is originally oriented at 90° relative to the line along the propagation direction of the two laser beams, Figure 4(1). In the optical trapping system the erythrocyte is turning, Figure 4(2), to the orientation at 180°, where it is stably trapped, Figure 4(3), in accordance with the torque calculation presented in Figure 3. The experimental results, Figure 4 (bottom row), corresponding to the erythrocyte's orientation, are in excellent agreement with the simulation.

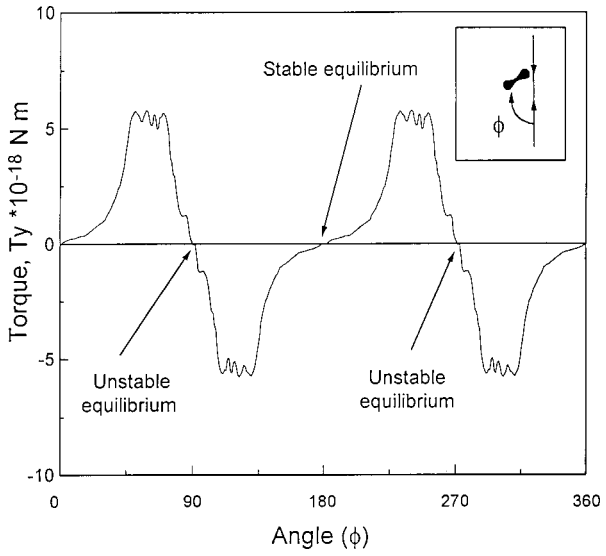

Fig. 3 Torque exerted on an erythrocyte vs the angle of the cell in a dual-beam trapping system. Unstable and stable equilibrium positions as shown. The inset defines the angle ϕ.

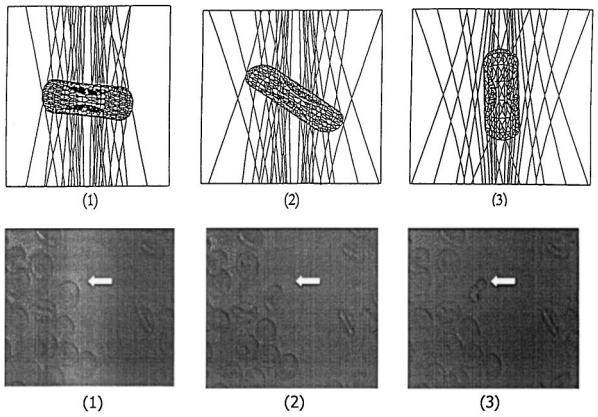

Fig. 4 Results of theoretical modeling (top row) and experimental results (bottom row) showing an erythrocyte before trapping (1), during reorientation in a dual-beam optical trap (2), and after the stable trapping is achieved (3).

Once a single cell is trapped and oriented, the beam(s) can be displaced relative to the medium surrounding the cell and, as a result, the trapped cell will follow the beam. Stable manipulation of the trapped cell at a constant velocity can be achieved if the drag force is in the equilibrium with the radiation pressure force. The equation of motion of the trapped cell can be expressed as follows:

$$ma = F - \gamma v, \tag{3}$$

where v is the maximum velocity of the cell which is displaced by a given force F and γ is the so-called drag coefficient, or damping factor. At low Reynold's numbers, the damping factor or drag coefficient can be estimated by approximating the disk shape of erythrocyte by a sphere of the same cross-sectional area:[23,24]

$$\gamma = 3\pi\eta D. \tag{4}$$

Here, η is the viscosity of the solution (water based, 1.02×10^{-3} Ns/m^2), and D is the diameter of the corresponding cross-sectional area of the cell. Stable manipulation of the trapped cell at a constant velocity can be achieved if the drag force is in equilibrium with the radiation pressure force, and the velocity is equal to the force divided by the damping factor $v = F/\gamma$. We examined two possible translations of the blood cell—one with the maximum cross section, and the other with the minimum cross section in the direction of the manipulation. The force was computed versus the offset of the cell center and beam axis, and is shown in Figure 5. From this graph the maximum velocity at which the cell can be translated was estimated to be 29 μm/s. These data are in agreement with the previous calculation on polystyrene spheres with similar characteristics[25] and serve as an approximation for establishing the displacement properties of erythrocytes during micromanipulation.

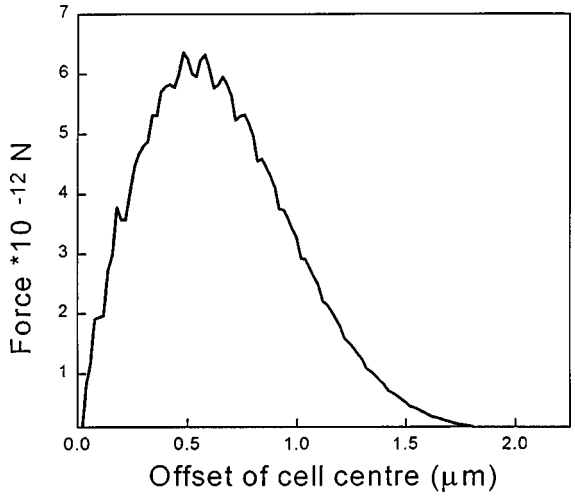

Fig. 5 Force of the optical-trapping system vs the offset of the cell center in the *Z* direction for an erythrocyte in a dual-beam trapping system. A maximum in the displacement defines the equilibrium location of the cell.

4 Trapping of Erythrocytes in Optical Tweezers: Design, Absorption Properties, and Thermal Effects

The single-beam trap was tested with latex microspheres prior to the trials with blood samples. Trapping of latex microspheres of diameter 7–14 μm in the single-beam trap was successfully accomplished at power densities of 300 and 20 kW/cm^2, with cw Ar-ion and He–Ne lasers, respectively. The spheres were seen to trap stably, and were easily micromanipulated at speeds higher than 50 μm/s.

The cellular constituents of peripheral blood differ from these latex micro-objects in many ways that may cause them to have a different trapping behavior, including the following:[19] blood cells are (1) membrane-enclosed structures which will pierce if exposed to high-power densities; (2) heterogeneous in refractive index; (3) heterogeneous and more irregular in shape; and (4) colored, and will absorb different light wavelengths, depending upon their composition. The absorption coefficient of erythrocytes is strongly dependent on wavelength and can be a limiting factor in the performance of an optical-trapping system used on biological systems. Assessment of the absorption of light of various wavelengths by erythrocytes can be accomplished by taking into account the absorption of the predominant molecular and macromolecular components of the erythrocyte cytoplasm, namely, water and hemoglobin, respectively. Water absorption at both of these visible wavelengths is infinitesimal, but hemoglobin absorption is an order of magnitude higher at 514.5 nm than at 632.8 nm.[26,27] Indeed, the use of the He–Ne laser for erythrocyte trapping even yields certain specific advantages over lasers in the near-infrared region. First, absorption of water is considerably lower in visible wavelengths when compared to infrared or near-infrared wavelengths. As well, the absorption of oxyhemoglobin is lower at 632.8 nm than at near-infrared wavelengths. Modeling of the optical trapping system performed for nonabsorbing erythrocytes and for erythrocytes having an absorption equal to that of hemoglobin at 632.8 nm showed that the effect of hemoglobin absorption on erythrocyte trapping was negligible. While these differences in absorption may not affect trapping, in terms of ease of trapping and orientation of trapped cells, their role in photodamage has not been well established.[26]

Trapping of erythrocytes using a high-power cw Ar-ion laser in the single-beam trap was hindered by the fragility of the erythrocytes, which were seen to visibly expand in the heat at the focus of the objective and shear due to the small focal spot generated by the 100×1.25 NA objective. While trapping and manipulation of erythrocytes without cell deformation were attained using a 35 mW He–Ne laser focused using the same 100×1.25 NA objective, photostress effects leading to morphologically visible deformation of the cells were still evident in a significant proportion of cells trapped. Erythrocytes that were trapped oriented themselves with their longest axis parallel to the direction of propagation of the beam, as seen previously in the literature,[28] and as predicted by the modeling results.

Absorption in the focus of a microscope objective may also cause unwanted heating of the surrounding medium, water, which would affect erythrocytes. Estimates confirmed by experimental results demonstrate that the temperature increase in a focus of a microscope objective can reach 3 K with NA $=1.3$ objective.[29,30] Since the power of the laser beam entirely determines the gradient force of trapping, the alternative method of using the scattering force of two beams counterpropagating through low-magnification microscope objectives would be beneficial in reducing the intensity in the trapping region. The use of low-magnification, high-focal-range objectives thus reduces photodamage, since the power density in the trapping region is considerably reduced. Furthermore, the low-magnification microscope objectives have larger focal distances than those with high magnification, increasing the working range of the system.

Using the dual-beam trap described above, erythrocytes were trapped at 15 mW of input power. As suggested by modeling studies, and as with the single-beam trap, trapped erythrocytes are oriented in the dual beam with their longest axis parallel to the direction of propagation of the beams. No morphological photostress effects were exhibited even after erythrocytes were trapped and micromanipulated for periods exceeding 20 min.

5 Image-Processing System and Automation of Single-Cell Sorting

Identification of single cells constitutes the basis for developing a cell sorting system. In medical laboratories, staining or immunological techniques are used to assist in identification of cell types.[19] As it is required that the single-cell sorting system be as nondestructive as possible to the sample, these techniques may not be feasible. Nonetheless, an identification of blood cells can be based on the morphological characteristics of unstained cells, including size, shape, and color.[31] In the single-cell sorting system, cells are sized on the basis of their longest dimension (as erythrocytes may be found in many orientations but, because of their radial symmetry, maintain a constant longest dimension). A micrometric grid can be placed onto the sample holder in order to calibrate the sizes; alternatively, a statistical estimate of cell sizes assuming that the erythrocyte lengths are most common, can be

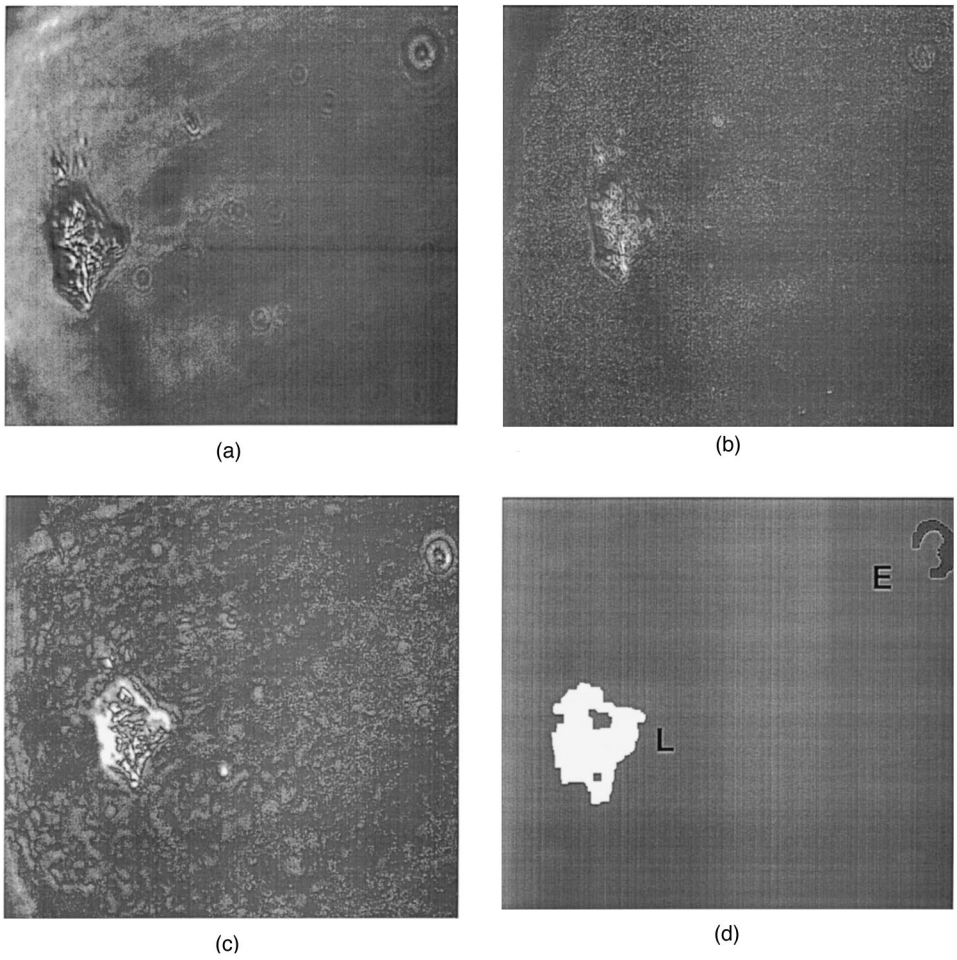

Fig. 6 Original image (a) shows cells comparable in size and shape to an erythrocyte (E) and a leukocyte (L), respectively. Image processing involves thresholding (b) and background subtraction (c), followed by edge enhancement. The automated cell identification program identifies the cells on the basis of their sizes as an erythrocyte (red) and a leukocyte (white), respectively, and can locate their relative positions as shown in (d).

used for calibration. While there is a definite degree of overlap in the sizes of the cellular constituents of peripheral blood, one is still able to roughly identify particles on the basis of the longest dimension.

We have applied several image-processing algorithms for single-cell identification. Detection of cells in an image containing these objects and a background can be achieved by using a simple thresholding technique.[32] In this method, which is used in many image-processing systems, all areas with intensity above a certain threshold value are assigned to the objects. However, due to nonuniformities in the background the image may possess some irregularities or bright areas, which do not belong to the object but can be assigned to it if this technique is used alone. This ambiguity is removed by combining this method with a technique involving background subtraction, wherein the image is assumed to be comprised of the two main categories—the background and the object; the latter is obtained by subtracting the background image from the original image. The quality of the image of the object can be further refined by analyzing the changes in intensity between the original image and the background image. This method works best if the background is not affected by subtraction of the image of the object, which is not always feasible due to the possibility of nonhomogeneous illumination of the background upon which the cells are imaged. In addition, an edge-enhancement technique can be used to improve the quality of the boundaries of the object. Each pixel and its neighboring pixels are multiplied by a matrix[33] to enhance the gap in intensity values of the pixels between the object and the background, providing stronger contours of the object's boundaries. In order for the pixels belonging to the object to be connected together, the image can be dilated (that is, assignment to the object the areas containing some of the background pixels completely surrounded by object's pixels), and further eroded (that is, assignment back to the background pixels that were not completely surrounded by the object) to set the object back to its original size.[34] After a cell is detected, it can be identified based upon its size and morphological characteristics.

The image-processing algorithm developed as part of our single-cell sorting system used all of the above-described image-processing techniques combined together. Results of this image-processing and recognition techniques are shown in Figure 6 for a real image (a) of two cells comparable in size and shape to an erythrocyte and a leukocyte, respectively. Thresholding and background subtraction images are shown

in Figures 6(b) and 6(c), respectively. As seen in Figure 6(d), the image-processing system identified and spatially positioned both cells. We note that as there may be a difference between the plane of focus of the trapped cell and the plane of the surrounding cells, the apparent sizes of these cells may differ from their actual sizes. As a result, identification may be restricted only to imaged cells that are in focus. The system can identify erythrocytes that are in focus and can differentiate them from leukocytes 100% of the time.

If this is applied to the cell to be sorted, the result is a procedure allowing both for single-cell identification and sorting. In order to automate such an identification procedure, the video output from the charge-coupled-device (CCD) camera used in the optical trapping setup was sent to a computer fitted with a program allowing for identification of cells using size as the defining criterion.

6 Automated Manipulation of Erythrocytes

Automated cell manipulation is obtained if micromanipulation of the identified and trapped cell is achieved through motorized stages controlled by a computer able to give a series of commands for the manipulation. In the dual-beam configuration, a trapped erythrocyte always maintained its longest axis along the direction of beam propagation. It can be manipulated relative to its environment, if the entire sample is moved by micrometric amounts while the cell is trapped.

The rate of sorting is dependent on the relative velocity of manipulation and on the distance between compartments. We have achieved relative manipulation velocities of greater than 20 μm/s for erythrocytes using the dual-beam trap. With automated control, at approximately 3 μm/s, erythrocytes have been seen to remain trapped when manipulated in the plane of trapping for up to 20 min. Figure 7 shows an erythrocyte being manipulated in a path exceeding 1 mm in length, with automated control of the motion. As can be seen in Figure 7, the majority of cells in the sample have settled on the bottom surface of the sample holder, and are defocused relative to the trapped erythrocyte, meaning that the two are in different planes.

As mentioned earlier, the dual-beam trap is advantageous because of the lesser power density and, as a consequence, the lesser photostress effects on cells in the trapping region. In addition, this configuration has a larger working range in three dimensions, due to the large depth of focus of the low-magnification objectives used, which is on the order of millimeters compared to micrometers for the 100$\times$ objective. This yields a specific advantage in sorting applications as manipulation of the trapped cell in three dimensions is possible. We have performed out-of-plane manipulation of an erythrocyte when the trapping region was translated in the Z direction by synchronously moving the two counterpropagating beams. The erythrocyte was then manipulated in an XY plane devoid of the other cells. Since the majority of cells in a given sample will have settled to the bottom surface, by changing the relative distance between the plane of the foci of both beams in the trap and the bottom surface of a sample, one can lift a trapped cell and manipulate it freely in a plane devoid of other cells, thus preventing sorting complications due to cell–cell interactions.

The sorting technique is completed with the cell being manipulated into a given volume which is designated to hold that particular cell type. Algorithms for the construction of a separation path that minimize cell–cell contact and prevent other cells from entering into the trap have been described in the literature.[14] The designated volumes for the cells must be housed in a structure compartmentalized in such a fashion that flow between volumes is negligible.[14] Mechanical barriers, such as doors and distance, as well as chemical barriers to cell interaction, have been theorized. Gels which liquefy or alter their properties when exposed to either the light or the heat of the beam focus can potentially be used as chemical barriers between such compartments.

7 Medical Applications

All-optical manipulation and sorting of single cells have definite specific applications in medical diagnostics and therapy. The single-cell sorter is well suited for the recovery of rare cells from aqueous solutions. Cell sorting techniques based upon optical trapping and micromanipulation provide a threefold advantage over conventional cell sorters, such as fluorescence-activated cell sorters, magnetic-based cell sorters, and immunoadsorption columns.[13] First, conventional cell sorters work on the bulk scale, whereas cell sorters based on optical trapping have the capability of sorting single cells, reducing the sample size required. Second, the cell sorters based on optical trapping have a high positional accuracy compared to traditional cell sorters, which typically manipulate a volume of fluid containing a particular cell rather than the cell itself. Finally, sorting based upon optical trapping is a completely sterile procedure, as there is no direct contact with the cells to be sorted, and the sorting procedure can even be used for samples in completely enclosed containers.[14] The harvesting of hematopoetic stem cells from umbilical cord blood for use in gene therapy, for example, could be achieved provided the stem cells can be identified and trapped.[13,35]

When combined with the tools of the molecular biology laboratory, which, with the advent of the polymerase chain reaction (PCR), allow for the use of picograms of DNA in sequencing and analysis,[36] the single-cell sorter becomes a novel tool in genetic screening and analysis which can be incorporated into lab-on-a-chip applications. Optical trapping of an identified cell, followed by manipulation, DNA recovery, and single-cell PCR, would allow for the genetic screening of the cells. This can be easily combined with laser microbeam microdissection methods to facilitate the single-cell preparation of pathological specimens for genetic analysis.[37] The sterile nature of the manipulation again yields considerable advantages for this application, as molecular techniques are generally of high sensitivity and require clean sample preparation.[37]

One potential diagnostic assay resulting from the combination of single-cell sorting and molecular analysis has been identified, namely, the genetic analysis of fetuses using fetal cells found in maternal circulation.[36,38] Fetal nucleated erythrocytes, which cross the placenta into maternal circulation, if identifiable, could readily be sorted. Through the use of single-cell PCR, the cells could be genetically analyzed on the single-cell or few-cell levels. This would allow for the genetic screening and sex determination of fetuses using only the

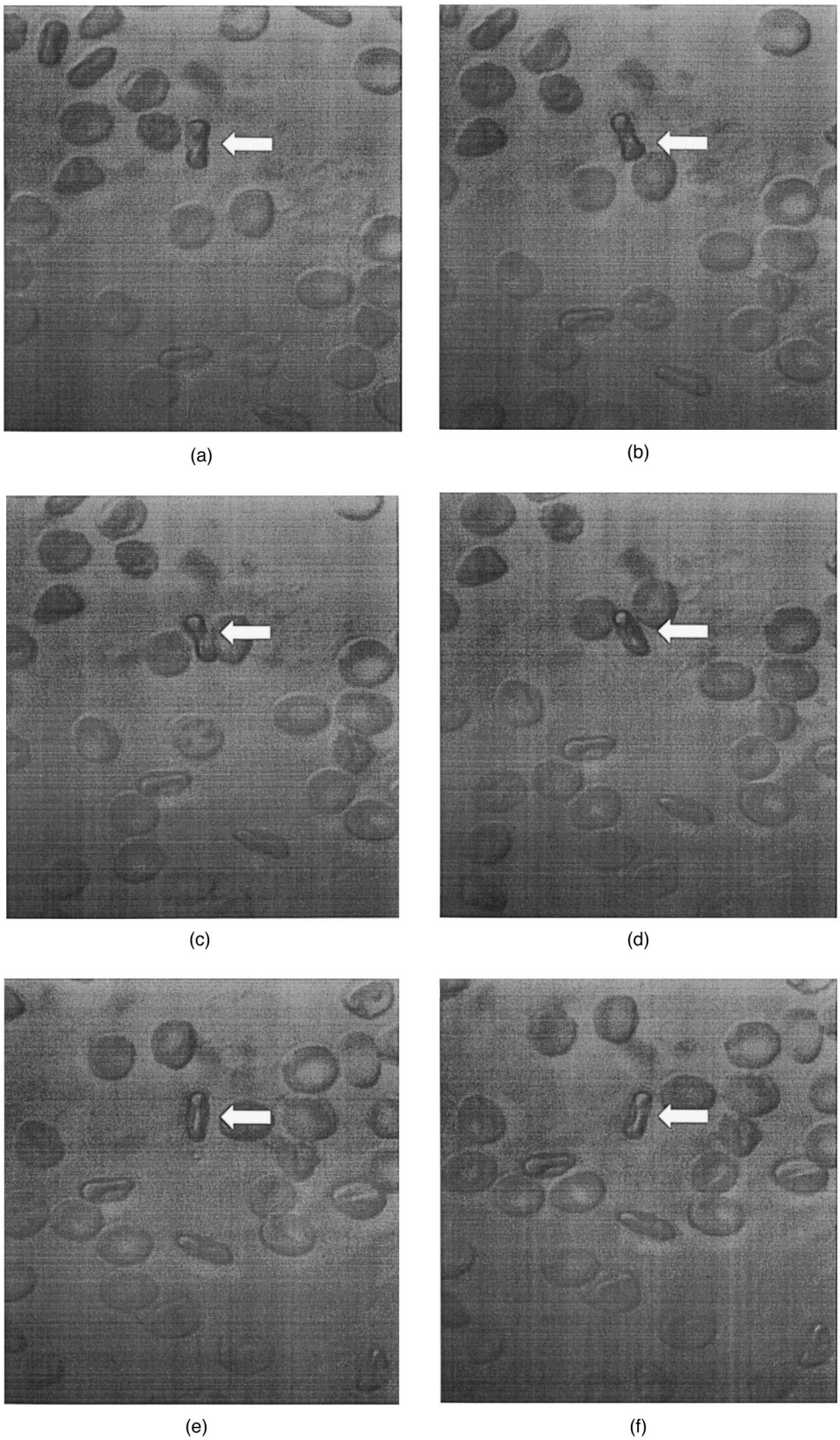

Fig. 7 Series of six images showing the automated manipulation of an erythrocyte over a distance of 30 μm using the dual-beam optical trap. Automated manipulation occurred at velocities of up to 3 μm/s.

amount of blood in a pinprick, eliminating the danger of chorionic villus sampling and amniocentesis, which induce complications at the rates of 1.0% and 0.5%, respectively.[36,39]

The possibility of the use of erythrocytes in targeted drug delivery has been a subject of extensive research, by virtue of their numbers and long lifetimes in circulation.[40] It has been proposed that the linkage of drug pharmacophores to the erythrocyte surface, for example, by covalent linkage to membrane proteins, would significantly enhance the pharmacokinetics of delivery, specifically by increasing the half life and controlling the volume of distribution of the drug.[40] The ease of manipulation and control of the position of individual erythrocytes of our system make it an ideal adjunct to the making and characterization of such pharmacophore–erythrocyte complexes.

The automated cell sorting system can also be used in the creation of cell patterns and biosensors.[41,42] One such application is the use of cell patterns in drug screening, which is one of the most expensive steps in drug development, and is often subject to ethical concerns, as animals are often used for the screening process.[41] The use of cell biosensors in drug screening will allow for the determination of the effects of drugs at the cellular level. The creation of such cell patterns is dependent upon the ability to spatially locate a cell of a particular type into the array or other pattern, analogous to the definition of sorting presented earlier. The ability to automate such a procedure is of benefit in facilitating the production of such biosensors, making it another potential application area for the automated single-cell sorting system.

In addition, optical trapping has become routine in a number of research applications in medicine and cell biology. Immunoassays based upon the laser power required to break an antibody–antigen complex using optical tweezers have been developed to allow the detection of femtomolar concentration of an antigen. Laser-assisted *in vitro* fertilization has been achieved using optical trapping.[37] Optical trapping has also been incorporated in other research applications, including assessment of the physics of mechanoenzymes,[5,6] micromanipulation for microsurgery,[37] DNA stretching,[43] and single-molecule enzymatic modification of DNA.[44]

8 Conclusions

An automated single-cell sorting technique has been developed based on single- and dual-beam optical traps, the latter preferred due to lesser photodamage to sorted cells, and the increased ability to move cells in three dimensions. Using human peripheral blood as a model system, an automated cell identification based on size was developed, and used to sort erythrocytes from the other cellular components of peripheral blood. The single-cell sorting system includes an automated imaging-processing system that allows for cells to be identified prior to the manipulation. We have successfully manipulated erythrocytes for distances greater than 1 mm and for times longer than 20 min using the automated dual-beam trap, without morphologically visible photodamage. As a corollary, the behaviors of human erythrocytes in single- and dual-beam optical traps have been theoretically calculated using a modeling program, and experimentally verified.

Our single-cell sorter fits into a niche of cell sorting that cannot be achieved by conventional methods, including flow cytometry. Our sorter allows for a greater positional control of the location of sorted cells, and allows for the manipulation of cells in a noncontact, sterile manner. The cell sorter can be used to construct cell patterns for biosensors and other lab-on-a-chip applications. Our single-cell sorting system is thus well suited to a number of applications in medical diagnostics and therapy, and, when incorporated with the techniques of the molecular biology laboratory, has the potential to become a novel technique for genetic screening and diagnosis.

Acknowledgments

The authors would like to thank D. McDermid for help in the writing and testing of cell identification programs, and M. Ashman for providing technical help and helpful discussions on the optical-trapping systems. The authors would also like to thank P. L'Abbe for helpful discussions on the construction of sample holders, and the Ottawa Ethics Board for approving the use of human blood for this project. One of the authors (S.C.G.), a medical student, would like to thank the Faculty of Medicine of the University of Toronto and the Jane and Howard Jones Bursary for funding this research project. One of the authors (C.P.G.) is a Fellow SPIE. The Optics Group at INMS and the Department of Physics and Astronomy at Laurentian University would also like to thank the Faculty of Medicine of the University of Toronto for allowing this unique collaboration in the field of biomedical optics.

References

1. A. Ashkin, ''Acceleration and trapping of particles by radiation pressure,'' *Phys. Rev. Lett.* **24**, 156–159 (1970).
2. W. H. Wright, G. J. Sonek, and M. W. Berns, ''Parametric study of the forces on microspheres held by optical tweezers,'' *Appl. Opt.* **33**(9), 1735–1748 (1994).
3. A. Ashkin, J. M. Dziedzic, J. E. Bjorkholm, and S. Chu, ''Observation of a single-beam gradient-force optical trap for dielectric particles,'' *Opt. Lett.* **11**, 288–290 (1986).
4. A. Ashkin, J. M. Dziedzic, and T. Yamane, ''Optical trapping and manipulation of single cells using infrared laser beams,'' *Nature (London)* **330**, 769–771 (1987).
5. K. Svoboda, C. F. Schmidt, B. J. Schnapp, and S. M. Block, ''Direct observation of kinesin stepping by optical-trapping interferometry,'' *Nature (London)* **365**, 721–727 (1993).
6. N. Thomas and R. A. Thornhill, ''The physics of biological molecular motors,'' *J. Phys. D* **31**, 253–266 (1998).
7. R. Steubing, S. Cheng, W. H. Wright, Y. Numajiri, and M. W. Berns, ''Laser-induced cell fusion in combination with optical tweezers: The laser-cell fusion trap,'' *Cytometry* **12**, 505–510 (1991).
8. H. Liang, W. H. Wright, S. Cheng, W. He, and M. W. Berns, ''Micromanipulation of chromosomes in PTK2 cells using laser microsurgery (optical scalpel) in combination with laser-induced optical forces (optical tweezers),'' *Exp. Cell Res.* **204**, 110–120 (1993).
9. Y. Tadir, W. H. Wright, O. Vafa, T. Ord, R. H. Asch, and M. W. Berns, ''Micromanipulation of sperm by laser-generated optical trap,'' *Fertil. Steril.* **52**, 870 (1989).
10. D. T. Chiu, S. J. Lillard, R. H. Scheller, R. N. Zare, S. E. Rodriguez-Cruz, E. R. Williams, O. Orwar, M. Sandberg, and J. A. Lundqvist, ''Probing single-secretory vesicles with capillary electrophoresis,'' *Science* **279**, 1190–1193 (1998).
11. B. B. Riley, C. Zhu, C. Janetopoulos, and K. J. Aufderheide, ''A critical period of ear development controlled by distinct populations of ciliated cells in the zebrafish,'' *Dev. Biol.* **191**, 191–201 (1997).
12. S. Seeger, S. Monajembashi, K. J. Hutter, G. Futterman, J. Wolfrum, and K. O. Greulich, ''Application of laser optical tweezers in immunology and molecular genetics,'' *Cytometry* **12**, 497–504 (1991).
13. F. Beaujean, ''Methods of CD34+cell separation: Comparative analysis,'' *Transfus. Sci.* **18**(2), 251–261 (1997).
14. T. N. Buican, *Cell Separation, Science and Technology*, American Chemical Society, Washington, DC, pp. 58–72 (1991).

15. P. J. H. Bronhorst, G. J. Streekstra, J. Grimbergen, E. J. Nijhof, and J. J. Sixma, ''A new method to study shape recovery of red blood cells using multiple trapping,'' *Biophys. J.* **69**, 1666–1673 (1995).
16. A. Elgsaeter, B. T. Stokke, A. Mikkelsen, and D. Branton, ''The molecular basis of erythrocyte shape,'' *Science* **234**, 1217–1223 (1986).
17. P. Zachee, J. Snauwaert, P. Vandenberghe, L. Hellemans, and M. Boogaerts, ''Imaging of red blood cells with the atomic-force microscope,'' *Br. J. Haematol.* **95**, 472–481 (1996).
18. A. Roggan, M. Friebel, K. Dorschel, A. Hahn, and G. Muller, ''Optical properties of circulating human blood in the wavelength range 400–2500 nm,'' *J. Biomed. Opt.* **4**(1), 36–46 (1999).
19. W. R. Platt, *Color Atlas and Textbook of Hematology*, Pitman Medical, London (1969).
20. A. Ashkin, ''Forces of a single-beam gradient laser trap on a dielectric sphere in the ray-optics regime,'' *Biophys. J.* **61**, 569–582 (1992).
21. W. Wang, A. E. Chiou, G. J. Sonek, and M. W. Berns, ''Self-aligned dual-beam optical-laser trap using photorefractive-phase conjugation,'' *J. Opt. Soc. Am. B* **14**(4), 697–705 (1997).
22. R. C. Gauthier, ''Theoretical investigation of the optical trapping force and torque on cylindrical micro-objects,'' *J. Opt. Soc. Am. B* **14**(12), 3323–3333 (1997).
23. N. Curle, H. J. Davies, *Modern Fluid Dynamics*, Van Nostrand, Princeton, New Jersey (1968).
24. G. K. Batchelor, *An Introduction to Fluid Dynamics*, Cambridge University Press, Cambridge (1967).
25. T. C. Bakker Schut, E. F. Schipper, B. G. de Groot, and J. Greve, ''Optical-trapping micromanipulation using 780 nm diode lasers,'' *Opt. Lett.* **18**, 447–449 (1993).
26. K. Svoboda and S. M. Block, ''Biological applications of optical forces,'' *Annu. Rev. Biophys. Biomol. Struct.* **23**, 247–285 (1994).
27. S. T. Flock, B. C. Wilson, and M. S. Patterson, ''Total attenuation coefficients and scattering phase functions of tissue and phantom materials at 633 nm,'' *Med. Phys.* **14**(4), 835–841 (1987).
28. S. Sato, M. Ishigure, and H. Inaba, ''Optical trapping and rotational manipulation of microscopic particles and biological cells using higher-order-mode Nd:YAG laser beams,'' *Electron. Lett.* **27**, 1831–1832 (1991).
29. A. Schonle and S. W. Hell, ''Heating by absorption in the focus of an objective lens,'' *Opt. Lett.* **23**, 325–327 (1998).
30. A. Sennaroglu, ''Quantitative study of laser-beam propagation in a thermally loaded absorber,'' *J. Opt. Soc. Am. B* **14**(2), 356–364 (1997).
31. J. K. Mui and K. S. Fu, *Automated Classification of Nucleated Blood Cells Using Digital Image Processing Techniques*, Comptex Scientific, New York (1978).
32. J. R. Weaver and J. L. S. Au, ''Application of automatic thresholding in image analysis scoring of cells in human solid tumors labeled for proliferation markers,'' *Cytometry* **29**, 128–136 (1997).
33. R. C. Gonzalez and P. Wintz, *Digital Image Processing*, Addison-Wesley, Reading, Massachusetts (1992).
34. C. R. Giardina and E. R. Dougherty, *Morphological Methods in Image and Signal Processing*, Prentice-Hall, Englewood Cliffs, New Jersey (1988).
35. D. S. Krause, M. J. Fackler, C. I. Civin, and W. S. Ma, ''CD34 structure and clinical utility,'' *Blood* **87**, 1–13 (1996).
36. R. Stevenson, ''PCR and optical trapping may team up for single-cell genetic screening,'' *Am. Biotechnol. Lab.* **9**(9), 14–15 (1991).
37. K. Schutze, H. Posl, and G. Lahr, ''Laser micromanipulation systems as universal tools in cellular and molecular biology and in medicine,'' *Cell. Mol. Biol.* **44**(5), 735–746 (1998).
38. D. W. Bianchi, J. M. Williams, L. M. Sullivan, F. W. Hanson, K. W. Klinger, and A. P. Shuber, ''PCR quantitation of fetal cells in maternal blood in normal and aneuploid pregnancies,'' *Am. J. Hum. Genet.* **61**, 822–829 (1997).
39. K. Sundberg, J. Bang, S. Smidt-Jensen, V. Brocks, C. Lundsteen, J. Parner, N. Keiding, and J. Philip, ''Randomized study of risk of fetal loss related to early amniocentesis versus chorionic villus sampling,'' *Lancet* **350**, 697–703 (1997).
40. A. Krantz, ''Red-cell-mediated therapy: Opportunities and challenges,'' *Blood Cells Mol. Dis.* **23**(3), 58–68 (1997).
41. M. Zahn and S. Seeger, ''Optical tweezers in pharmacology,'' *Cell. Mol. Biol.* **44**, 747–761 (1998).
42. M. Zahn, J. Renken, and S. Seeger, ''Fluorimetric multiparameter cell assay at the single-cell level fabricated by optical tweezers,'' *FEBS Lett.* **443**, 337–340 (1999).
43. J. Dapprich, ''Single-molecule DNA digestion by lambda exonuclease,'' *Cytometry* **36**(3), 163–168 (1999).
44. T. T. Perkins, D. E. Smith, R. G. Larson, and S. Chu, ''Stretching of a single tethered polymer in a uniform flow,'' *Science* **268**, 83–86 (1995).